PREDICTING FLOOD INUNDATION IN OWERR IMO STATE USING HYDRAULIC MODEL

E C Abara, En Ossai, Igbokwe, J.I

PREDICTING FLOOD INUNDATION IN OWERR IMO STATE USING HYDRAULIC MODEL

Abara, E.C., Ossai, E.N., and Igbokwe, J.I.

Abstract- Flooding in Owerri, Imo State, is increasingly frequent and destructive, causing economic losses, displacement, and infrastructure damage. The city's low-lying topography, poor drainage, and rapid urbanization, which encroaches on natural floodplains, exacerbate the problem, revealing the inadequacy of current flood management efforts. Therefore, this study aimed at predicting flood inundation in Owerri Imo State using hydraulic model. The objectives of the study are to: examine the pattern and extent of landcover/landuse within the study area; determine the roughness coefficient of the various landcover/landuse; assess the surface runoff potential across the study area; and model the extent of flood vulnerability in the study area using HEC-RAS. This study employed a geospatial-hydraulic modeling approach to predict flood inundation across Owerri Municipal. Land cover/land use classification was derived from Sentinel imagery using supervised classification techniques in QGIS, achieving high accuracy with an overall classification accuracy of 96.6% and a Kappa coefficient of 0.949. Each land cover class was assigned a corresponding Manning's roughness coefficient and rasterized for hydraulic simulation. Surface runoff potential was estimated using the SCS-Curve Number method, integrating land cover data and soil hydrologic groups (HYSOGs), while a high-resolution Digital Elevation Model (DEM) supported terrain analysis. Flood modeling was implemented using HEC-RAS 2D rain-on-grid simulations based on an extreme rainfall scenario of 3391.2 mm. Flood depth outputs were further classified into vulnerability zones. Exposure analyses were conducted by overlaying the vulnerability map with road networks and land use categories to assess infrastructure susceptibility. The study found that built-up areas dominated land cover, occupying 61.07% of the area, while vegetation and water bodies accounted for only 5.91% and 0.81%, respectively. Manning's roughness mapping showed that low-resistance surfaces prevailed, contributing to rapid runoff. Using the SCS-Curve Number method, the average runoff depth from a 3391.2 mm rainfall event was estimated at 536.63 mm, with localized peaks reaching 3354.21 mm. HEC-RAS 2D simulation identified widespread inundation, with high vulnerability zones concentrated in low-lying urban centers. Exposure analysis showed that over 20 km of roads and more than 2700 hectares of land, particularly residential and bare land, fall within moderate to high flood risk areas. Given that only 5.91% of the study area is covered by vegetation, while over 61.07% is built-up, it is recommended that urban greening programs be implemented. Establishing vegetative buffers along waterways, open parks, and green belts in flood-prone zones will increase surface resistance (Manning's n) and reduce the velocity and volume of surface runoff. These measures would also enhance infiltration and provide ecological co-benefits.

Keywords: Flood inundation modeling, HEC-RAS, River bathymetry, Owerri, Manning's coefficient, Urban flood vulnerability, Hydraulic simulation

1. Introduction

Flooding remains one of the most frequent and destructive natural disasters globally, causing substantial economic losses, displacement of populations, and damage to critical infrastructure (Jonkman, 2005; Kundzewicz et al., 2014). Its devastating effects are particularly evident in developing countries, where rapid urbanization, poor land-use planning, and weak disaster preparedness systems increase vulnerability (Adger et al., 2005; Douglas et al., 2008). In Nigeria, flood events have become a recurring environmental hazard, especially in southeastern cities such as Owerri, where the frequency and magnitude of flooding are rising due to increased rainfall intensity, climate variability, and anthropogenic modifications of the natural landscape (Aderogba, 2012; Efe, 2011).

Owerri, the capital of Imo State, is situated in a low-lying region intersected by major rivers including the Otamiri and Nworie. These rivers often overflow during peak rainy seasons, inundating both residential and commercial areas (Nwilo, Olayinka, & Anifowose, 2012). Urban expansion has encroached on floodplains and

natural drainage corridors, while impervious surfaces have reduced infiltration and increased surface runoff (Ajibade, McBean, & Bezner-Kerr, 2013). Consequently, the region faces a persistent flood risk exacerbated by inadequate drainage infrastructure, haphazard urban development, and poor flood forecasting systems (Ishaya, Ifatimehin, & Okafor, 2009; Adelekan, 2010).

To address these challenges, hydraulic models such as HEC-HMS and HEC-RAS have emerged as robust tools for flood prediction and inundation mapping (Bates & De Roo, 2000; Vieux, 2004). These models simulate hydrological and hydraulic processes, enabling the prediction of runoff, water surface elevations, and flood extents. Their application, however, depends heavily on the availability of quality input data, particularly river bathymetry, which describes the depth and shape of riverbeds (Horritt & Bates, 2002). Bathymetric data are critical for defining cross-sectional geometry and understanding flow resistance, especially in urban settings with engineered and natural channels (Di Baldassarre et al., 2009).

Recent advancements in geospatial technologies and remote sensing have facilitated the acquisition and integration of high-resolution bathymetric and terrain data for flood modeling (Teng et al., 2017; Fonstad et al., 2013). Tools like LiDAR, sonar, and photogrammetry now allow for accurate digital elevation and riverbed modeling, which enhances the reliability of simulation outputs (Mandlburger et al., 2015). These technologies, when used in combination with hydraulic models, provide planners with vital spatial insights to guide flood risk management, infrastructure development, and emergency response strategies (Pereira et al., 2017; Smith et al., 2012).

Despite these technological advancements, many cities in Nigeria, including Owerri, lack spatially explicit flood prediction frameworks. Existing flood risk assessments often rely on static maps or coarse data, limiting their usefulness for proactive planning (Ologunorisa & Abawua, 2005; Adeoye, Ayanlade, & Babatimehin, 2009). This study seeks to bridge that gap by applying a hydraulic modeling approach integrated with river bathymetry and geospatial analysis to simulate flood inundation patterns in Owerri. The outcome will support local stakeholders in identifying high-risk zones, designing mitigation interventions, and enhancing community resilience against future flood events.

2. Materials and Methods

2.1. Data Requirement and Sources

The study relied on both primary and secondary data to achieve its objectives. Remotely sensed satellite data from the Sentinel-2 MultiSpectral Instrument (MSI) with 10 m spatial resolution were used for land cover classification. This dataset was selected for its temporal frequency and high spectral resolution suitable for detecting urban, vegetation, and hydrological features.

A Digital Elevation Model (DEM) was obtained from the Shuttle Radar Topography Mission (SRTM) at a 30 m spatial resolution. This was used for terrain modeling, hydrological preprocessing, and floodplain extraction. In areas where higher resolution was needed, the DEM was resampled or enhanced using interpolation techniques.

Meteorological data, including daily rainfall time series for a 10-year period (2014–2024), were collected from the Nigerian Meteorological Agency (NiMet), while streamflow data and river cross-section measurements and drainage networks were extracted from the SRTM data. Field data were collected using GPS (Global Positioning System) to validate classified land cover types and assess existing flood-prone areas. Soil data were sourced from the FAO Harmonized World Soil Database.

2.2. Land Cover Classification and Analysis

Land cover classification is a critical step in flood modeling, as it influences both surface runoff behavior and hydraulic resistance across the landscape. To examine the pattern and extent of land cover and land use in Owerri Municipal, Sentinel-2 imagery was employed due to its high spatial resolution (10 meters for visible and near-infrared bands) and its suitability for detailed urban and environmental studies.

The Sentinel-2 Level-1C data were downloaded from the Copernicus Open Access Hub and preprocessed using the Sentinel Application Platform (SNAP). The preprocessing workflow involved atmospheric correction using the Sen2Cor processor, which transformed the Top-of-Atmosphere (TOA) reflectance into Bottom-of-Atmosphere (BOA) reflectance, removing atmospheric effects such as haze and water vapor. Other preprocessing tasks included band stacking, subsetting to the study area boundary (Owerri Municipal), and radiometric enhancement to improve visual and spectral interpretation.

Following preprocessing, a false color composite (Bands 8-4-3) was generated to enhance the separability of vegetation, built-up areas, water bodies, and bare surfaces. This served as the base for visual inspection and training sample selection. A supervised classification approach was then implemented using the Maximum Likelihood Classification (MLC) algorithm in the Semi-Automatic Classification Plugin (SCP) within QGIS 3.30. This algorithm was selected for its statistical robustness in handling normally distributed spectral data and for its widespread use in environmental modeling.

Training samples for the classification were derived from field observations, Google Earth Pro references, and high-resolution orthophotos. At least 20–30 training pixels were collected per class to ensure statistical validity. The land cover classes targeted for this study included:

1. Built-up areas (residential, commercial, industrial zones)
2. Vegetation (forests, shrubs, parks)
3. Agricultural land (cropland and mixed vegetation)
4. Bare surfaces (sandy, exposed soil)
5. Water bodies (rivers, ponds, flooded wetlands)

Post-classification processing was undertaken to improve the quality of the classified map. This included smoothing, clump removal, and majority filtering to eliminate salt-and-pepper noise and isolated misclassified pixels. These operations helped preserve spatial coherence and delineate realistic boundaries of land cover patches.

To evaluate the accuracy of the classification, an error matrix (confusion matrix) was generated by comparing classified pixels with independent validation samples derived from ground truth points and visual inspection in Google Earth Pro. The Overall Accuracy, Producer's Accuracy, User's Accuracy, and Kappa Coefficient were calculated to assess the performance of the classifier.

The final classified map was exported as a georeferenced raster in GeoTIFF format for further spatial analysis. This land cover dataset served multiple purposes:

1. It provided the basis for assigning Manning's roughness coefficients in the hydraulic model (Section 3.5);
2. It informed the Curve Number (CN) assignment in the runoff model (Section 3.6);
3. It supported spatial overlay for flood vulnerability assessment (Section 3.8).

Furthermore, spatial statistics such as the area coverage (in hectares) and percentage composition of each land cover class were computed to quantify the level of urbanization and vegetation cover within the study area. The temporal comparison with past classified images (e.g., Landsat data from 2000 or 2010) was also conducted to observe urban expansion trends and potential land use changes influencing flood risk.

The land cover classification process was meticulously executed to provide a reliable spatial framework for modeling hydrological and hydraulic processes in Owerri. The classification not only reflected the heterogeneity of land surface features but also enabled spatially distributed modeling of flood-generating mechanisms in the study area.

2.3. Determination of Roughness Coefficient (Manning's n)

The determination of Manning's roughness coefficient (n) is a crucial step in hydraulic modeling, as it quantifies the resistance offered by different land surfaces to the flow of water. This coefficient directly influences the velocity of water movement and the depth of inundation across both natural channels and overland floodplains. In this study, the roughness values were derived based on the classified land cover types generated in Section 3.4, supported by empirical literature, field observations, and expert judgment.

To achieve an accurate spatial representation of surface resistance, each of the five identified land cover classes—built-up areas, vegetation, agricultural land, bare surface, and water bodies—was assigned a typical Manning's n value. These values were based on standard hydraulic engineering references such as Chow (1959), Arcement and Schneider (1989), and USACE (2016) guidelines, which provide empirically derived roughness coefficients for different surface conditions. The selected values were then validated through visual inspection and limited in-situ field observations to ensure their applicability to the Owerri terrain.

To spatially integrate these roughness coefficients, the classified land cover raster was reclassified in QGIS using the Raster Calculator and reclassification tools. Each pixel of the land cover map was assigned its corresponding Manning's n value, resulting in a Manning's n raster layer that reflects spatial heterogeneity in surface roughness across the study area.

This raster layer was then exported in ASCII format and imported into HEC-RAS 6.3, where it was used to define roughness values across both the floodplain and channel domains in the 2D hydraulic modeling environment. In HEC-RAS, the terrain was divided into computational cells, and each cell inherited its Manning's n value from the spatial layer, ensuring that flow resistance was appropriately modeled at every location.

In areas where the river channels were explicitly defined (e.g., Otamiri River), a more detailed channel-specific Manning's n assignment was conducted using cross-sectional profiles derived from DEM and field data. For instance, riverbanks with vegetation were assigned slightly higher values than the main channel to reflect natural channel complexity.

During model calibration, sensitivity tests were conducted by adjusting the Manning's n values within their literature-defined ranges. This step assessed the influence of surface roughness on flood extent and depth, allowing the selection of optimal roughness values that produced results closely aligned with observed flood patterns.

Overall, the precise assignment and spatial modeling of Manning's n values in this study were instrumental in ensuring that the hydraulic simulations in HEC-RAS realistically represented the resistance to water movement within Owerri's heterogeneous landscape. The resulting outputs were used in subsequent stages of flood inundation prediction, floodplain delineation, and vulnerability mapping.

2.4. Surface Runoff Potential Modeling

Surface runoff modeling plays a pivotal role in flood prediction studies, as it determines the quantity of rainfall that does not infiltrate into the soil but instead flows over the surface, eventually contributing to streamflow and potential flooding. In this study, the surface runoff potential across Owerri was modeled using the Soil Conservation Service – Curve Number (SCS-CN) Method, which is widely adopted for hydrological modeling due to its simplicity, effectiveness, and compatibility with spatial datasets.

The SCS-CN method, developed by the U.S. Department of Agriculture Natural Resources Conservation Service (USDA-NRCS), estimates runoff depth from rainfall events based on land use, soil type, and antecedent moisture conditions. It requires the derivation of a Curve Number (CN), which is a dimensionless parameter that reflects the combined effect of land cover, soil infiltration capacity, and surface conditions.

The first step in the runoff modeling process was to prepare the input layers required for CN assignment: the land cover map derived in Section 3.4 and the soil hydrologic group (SHG) map obtained from the FAO Harmonized World Soil Database. The SHG map categorizes soils into four groups (A, B, C, D), where Group A soils have the highest infiltration capacity and Group D the lowest. In Owerri, predominant soils include sandy loams and clayey soils, falling mostly within Groups B, C, and D due to poor permeability and moderate to low infiltration rates.

These two layers were intersected in QGIS using the Raster Calculator and Zonal Statistics tools to generate a Composite Curve Number map, in which each pixel represented a unique CN value based on its land cover and soil type combination. The following formula was used:

$$Q = \frac{(P - 0.2S)^2}{(P + 0.8S)}, \quad \text{for } P > 0.2S$$

where:

Q = direct runoff (mm)

P = rainfall depth (mm)

S = potential maximum retention after runoff begins, calculated as:

$$S = \frac{25400}{CN} - 254$$

Using historical rainfall records (2014–2024) acquired from the Nigerian Meteorological Agency (NiMet), rainfall depths for selected extreme storm events (e.g., 2-year, 5-year, and 10-year return periods) were used to calculate runoff volume for each grid cell in the study area. These computations were automated in R programming environment to process large datasets efficiently and to simulate various rainfall scenarios.

In addition to CN-based runoff estimation, the terrain characteristics were also modeled using ArcGIS Spatial Analyst hydrology tools. The SRTM 30-meter resolution DEM was used to derive essential hydrological parameters, including:

1. Flow Direction: determines the direction of surface water movement based on elevation.
2. Flow Accumulation: identifies cells receiving the highest volume of upstream flow.
3. Slope: influences runoff velocity and erosion potential.
4. Watershed Delineation: defines sub-basins contributing to major rivers like Otamiri and Nworie.

These outputs were combined with the CN map and rainfall data to generate spatial runoff depth maps, identifying zones with high, moderate, and low runoff potential. Areas with high CN values, low slope, and impervious surfaces exhibited the highest runoff potential, posing a higher risk for surface flooding during intense rainfall events.

Furthermore, the runoff volumes computed were exported as hydrographs and used as inflow boundary conditions in the HEC-RAS model, enabling the hydraulic simulation to reflect realistic water volumes entering the river system and floodplain.

2.5. Hydraulic Flood Modeling with HEC-RAS

Hydraulic flood modeling represents the core component of this study, as it enables the simulation of water movement through river channels and across floodplains under varying hydrological conditions. The hydraulic model was developed using the Hydrologic Engineering Center's River Analysis System (HEC-RAS), version 6.3, which supports two-dimensional (2D) unsteady flow simulations. This version was selected for its enhanced capability in simulating surface water dynamics in complex terrain, including flow direction, depth, and velocity distribution across a spatial domain.

2.5.1. Data Preparation and Model Setup

The hydraulic modeling process began with the preparation of input datasets, most importantly the Digital Elevation Model (DEM), which serves as the foundation for terrain representation. The 30-meter Shuttle Radar Topography Mission (SRTM) DEM was first preprocessed to remove artifacts and fill sinks using the Fill tool in ArcGIS Hydrology toolbox. The DEM was then converted into a Triangulated Irregular Network (TIN) and raster terrain format required by HEC-RAS 2D modeling.

To define the river geometry and associated floodplain features, the preprocessed DEM was imported into HEC-GeoRAS, an ArcGIS extension used to extract and manage river geometry data for HEC-RAS. Within this environment, the following elements were manually digitized:

1. River centerlines for the Otamiri and Nworie rivers.
2. Flow paths and bank lines representing the left and right edges of riverbanks.
3. Cross-sectional cutlines perpendicular to the river centerline at regular intervals (typically every 100–200 meters).
4. Storage areas and inlets/outlets for wetlands and low-lying depressions.

This geometric information was exported in XML format and imported into the HEC-RAS geometry editor, where the river network and floodplain structure were defined. Each cross-section was assigned an appropriate Manning's roughness coefficient (n), based on the values derived in Section 3.5.

2.5.2. Boundary Conditions and Flow Inputs

Hydraulic simulation in HEC-RAS requires the specification of upstream and downstream boundary conditions to model the flow of water through the river system. At the upstream ends of the Otamiri and Nworie Rivers, inflow hydrographs were input as flow boundary conditions. These hydrographs were generated from the runoff estimates derived using the SCS-CN method in Section 3.6, based on historical rainfall events corresponding to 2-year, 5-year, and 10-year return periods.

At the downstream ends of the river system, normal depth conditions were applied to allow water to exit the simulation domain, based on calculated channel slopes and flow energy gradient. Internal boundary conditions such as lateral inflows and tributary confluences were also incorporated where minor drainage channels intersected the main river courses.

2.5.3. 2D Flow Area and Mesh Generation

The HEC-RAS 6.3 environment was used to define a 2D flow area covering the entire flood-prone region of Owerri. This 2D area was discretized using a computational mesh, which divides the terrain into smaller cells to solve the shallow water equations. The mesh size was optimized at 10 m × 10 m to balance computational efficiency with spatial resolution, especially in densely developed areas where finer resolution improves simulation accuracy.

Special attention was given to terrain breaklines such as roads, embankments, and levees, which were incorporated into the mesh to represent elevation discontinuities and flow barriers. These breaklines were essential in preserving topographic integrity and controlling flow routing within the urban floodplain.

2.5.4. Simulation and Execution of the Model

Once all geometry, flow data, and roughness coefficients were defined, the simulation was set up as an unsteady 2D flow model, using a computation time step of 1 to 5 seconds depending on flow stability and convergence requirements. The simulation period typically ranged from 6 to 24 hours to capture both peak flow and recession stages of flood events.

The model employed the full dynamic wave routing method, which solves the Saint-Venant equations for conservation of mass and momentum. This method accounts for backwater effects, flow reversals, and rapidly varying flows, which are commonly observed during urban flooding. The simulation outputs included:

1. Water surface elevation
2. Flood depth
3. Velocity magnitude
4. Inundation extent

These outputs were exported as georeferenced raster layers in GeoTIFF format and subsequently analyzed in QGIS to generate flood inundation maps.

3.7.6 Flood Scenario Simulation and Output Analysis

Three distinct flood scenarios were simulated based on storm return periods:

1. 2-year storm event (moderate flood)
2. 5-year storm event (severe flood)
3. 10-year storm event (extreme flood)

For each scenario, the resulting flood inundation maps were classified into depth categories such as:

1. Shallow flood (< 0.5 m)
2. Moderate flood (0.5 – 1.5 m)
3. Deep flood (> 1.5 m)

These maps provided critical spatial insights into which areas are most vulnerable to varying degrees of flood severity. Outputs were validated by overlaying with built-up areas, road networks, and public infrastructure to assess exposure and risk.

2.6. Flood Vulnerability Mapping and Zonation

Flood vulnerability mapping and zonation represent a crucial phase of this study, as they translate the hydraulic model outputs into actionable insights for urban flood risk management. This section describes how flood depth data, land use characteristics, population density, infrastructure exposure, and terrain factors

were integrated using Geographic Information System (GIS) techniques to delineate flood-prone areas and classify them based on levels of vulnerability.

2.6.1. Conceptual Framework of Vulnerability

In line with the United Nations Intergovernmental Panel on Climate Change (IPCC) framework, flood vulnerability is conceptualized as a function of exposure, sensitivity, and adaptive capacity. In this study, vulnerability was assessed spatially by integrating:

1. Exposure: areas physically located within flood zones, particularly those with residential, institutional, and commercial land uses.
2. Sensitivity: influenced by land cover type, drainage capacity, slope, and soil properties.
3. Adaptive capacity: considered indirectly through the presence or absence of formal drainage infrastructure and the density of the built environment.

A comprehensive flood vulnerability index was computed and mapped, by combining these elements in a GIS environment

2.6.2. Preparation of Flood Depth and Hazard Layers

The primary input for flood vulnerability mapping was the flood depth raster generated from the HEC-RAS simulations in Section 3.7. For each flood scenario (2-year, 5-year, and 10-year return periods), the flood depth outputs were imported into QGIS and reclassified into distinct depth categories based on severity:

1. Low flood depth: less than 0.5 meters
2. Moderate flood depth: 0.5 to 1.5 meters
3. High flood depth: greater than 1.5 meters

These reclassified rasters were used to generate flood hazard maps. The assumption was that areas with deeper flood depths represent higher hazard levels due to increased damage potential and longer recession time.

3. Results

3.1. Pattern and Extent of Landcover/Landuse in Owerri Municipal

The spatial distribution of land cover/land use (LULC) within Owerri Municipal was analyzed using classified raster data derived from Sentinel imagery. The classification delineated four major land cover types: Bare Land, Built-Up Area, Vegetation, and Water Body. These categories represent the dominant surface characteristics that influence hydrological responses such as infiltration, runoff, and flood susceptibility, see figure 1.

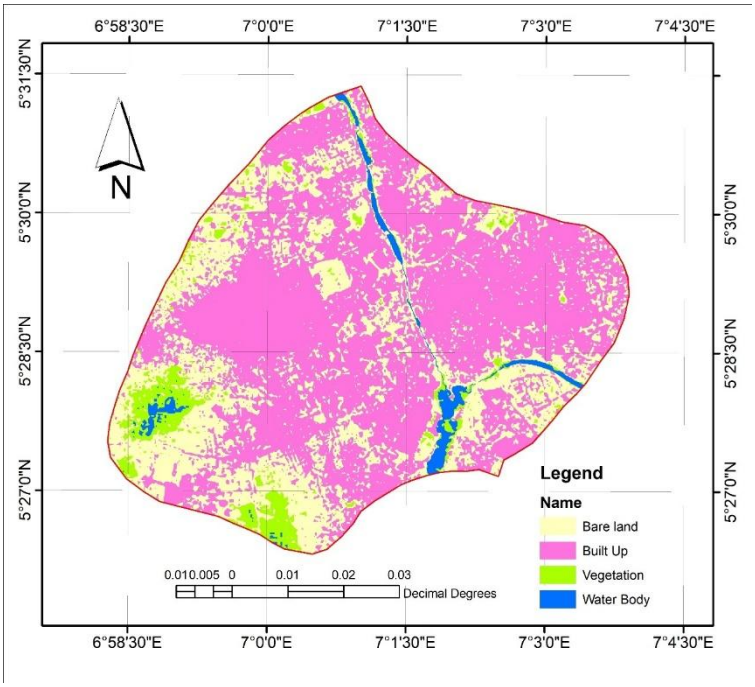

Figure 1: Landcover/Land Map of Owerri Municipal

The quantitative analysis reveals a significant dominance of Built-Up Areas, which occupy approximately 35.29 km², accounting for 61.07% of the total study area. This extensive coverage reflects the rapid urban development and population growth within Owerri, characterized by widespread construction of residential buildings, commercial infrastructure, and paved roads.

Following built-up areas, Bare Land covers 18.62 km² (32.21%). This class includes cleared lands, undeveloped plots, construction zones, and exposed soil areas, which contribute to increased surface runoff due to their reduced infiltration capacity.

Vegetation comprises 3.41 km² or 5.91% of the landscape. These areas represent remaining natural green cover, including trees, grasses, and scattered shrubs, mostly found on the city's periphery or along drainage corridors. While relatively small in extent, this class plays a crucial role in regulating microclimates and facilitating water infiltration.

Water Bodies, including ponds, minor rivers, and wetlands, occupy the smallest fraction of the landscape, with just 0.47 km² (0.81%). Despite their limited coverage, they are vital for natural drainage and flood attenuation. The distribution of these classes is shown in Table 1.

Table 4.1: Land Cover Types and Areal Extent in Owerri Municipal

Land Cover Type	Area (km²)	Percentage (%)
Built-Up Area	35.29	61.07
Bare Land	18.62	32.21

Vegetation	3.41	5.91
Water Body	0.47	0.81

This land use pattern reflects a landscape increasingly dominated by impervious surfaces, which poses challenges for stormwater absorption and increases the likelihood of urban flooding.

3.1.1. Classification Accuracy Evaluation

The classification accuracy of the land cover/land use map for Owerri Municipal was evaluated using both overall and class-specific accuracy metrics. These were derived from a comparison of the classified raster data against a reference dataset of 100 stratified random points, with 25 points allocated per land cover class. The results are summarized in table 2 and 3.

Table 4.2: Classification Accuracy Metrics

Metric	Value
Overall Accuracy (%)	96.6
Kappa Coefficient	0.949

Table 4.3: Producer's and User's Accuracy by Class

Land Cover Type	Producer's Accuracy (%)	User's Accuracy (%)
Bare Land	90.4	93.3
Built-Up Area	97.5	97.1
Vegetation	94.6	95.4
Water Body	100	100

The overall classification accuracy (table 4.2) was found to be 96.6%, indicating that the vast majority of classified pixels matched their corresponding reference values. This indicates that the spectral separation and classification algorithm applied were highly effective in distinguishing between the different land cover types present within the study area.

In addition to the overall accuracy, the Kappa Coefficient was computed as 0.949. The Kappa statistic adjusts for agreement that might occur by chance and provides a more robust measure of classification performance. A value of 0.949 falls within the "almost perfect agreement" range according to Landis and Koch (1977), further confirming the high reliability of the classification.

3.1.2. Class-Specific Accuracy Metrics

To evaluate the accuracy at the level of individual land cover classes, both Producer's Accuracy and User's Accuracy were calculated (table 4.4). These class-based metrics provide insights into the types of classification errors, such as omission (false negatives) and commission (false positives).

Bare Land achieved a Producer's Accuracy of 90.4%, indicating that 90.4% of the actual bare land areas were correctly identified in the classification. Its User's Accuracy of 93.3% indicates that 93.3% of the pixels classified as bare land were indeed bare land on the ground. The minor discrepancies are likely due to spectral similarities between bare soil and some impervious surfaces or mixed pixels at boundaries.

Built-Up Area exhibited very strong performance, with a Producer's Accuracy of 97.5% and a User's Accuracy of 97.1%. This means nearly all actual built-up areas were accurately captured, and pixels assigned to this class were correctly labeled with high confidence. This high accuracy can be attributed to the distinct spectral reflectance of rooftops and pavements in urban settings.

Vegetation recorded a Producer's Accuracy of 94.6% and a User's Accuracy of 95.4%. These results confirm that the classification effectively distinguished vegetated areas such as grasslands and shrubs from other land cover types, despite their sometimes-intermediate reflectance values.

Water Body achieved perfect classification performance, with both Producer's Accuracy and User's Accuracy at 100%. This indicates that all water body reference points were correctly identified, and no other land cover types were misclassified as water. This outcome is typical in regions where water surfaces are spectrally distinct and well-delineated from surrounding features.

3.2. Roughness Coefficient Assignment for Hydraulic Modeling

An essential aspect of hydraulic modeling is the accurate representation of surface roughness, which governs the resistance encountered by flowing water over different land cover types. In this study, Manning's roughness coefficient (n) was employed as the principal parameter for quantifying surface friction. Manning's *n* reflects the retardation effect exerted by terrain features such as vegetation, urban surfaces, soil textures, and water bodies on the velocity and energy of overland and channel flow.

Each land cover class identified from the classified land use/land cover (LULC) map of Owerri Municipal was systematically assigned a corresponding roughness coefficient based on standard hydrological references (e.g., Chow, 1959; Arcement and Schneider, 1989) and further refined through visual inspection of the study area using high-resolution satellite imagery and field observations. This approach ensured that the assigned values were both literature-consistent and context-specific, reflecting the physical characteristics of the terrain in Owerri.

The roughness coefficient values assigned to each land cover type are summarized in Table 44.

Table 4: Assigned Manning's n Values by Land Cover Type

Land Cover Type	Manning's n	Description
Built-Up Area	0.015	Includes roads, rooftops, and other impervious surfaces that offer minimal resistance to water flow due to their smooth, hardened nature.
Bare Land	0.020	Comprises open, unvegetated areas such as sandy soils, cleared lots, and construction sites, offering moderate flow resistance.
Vegetation	0.050	Encompasses grasslands, shrubs, and low-density woodland with high surface roughness that significantly slows down surface runoff.
Water Body	0.035	Consists of open water such as rivers and ponds with moderate frictional resistance, depending on flow depth and channel morphology.

These Manning's *n* values were rasterized in GIS by reclassifying the LULC raster based on the assigned coefficients. Each pixel in the land cover raster was converted to its corresponding roughness coefficient, resulting in a spatially distributed Manning's n raster layer.

This roughness raster (Figure 2) was then exported in GeoTIFF format and imported into the HEC-RAS 2D hydraulic modeling environment.

Integrating this layer into the hydraulic simulation enhanced the precision of water surface elevation estimations, flood depth calculations, and velocity distributions, especially in highly heterogeneous urban catchments such as Owerri. Consequently, the inclusion of this parameter significantly improved the fidelity of the model in replicating real-world hydrodynamic conditions under varying rainfall intensities.

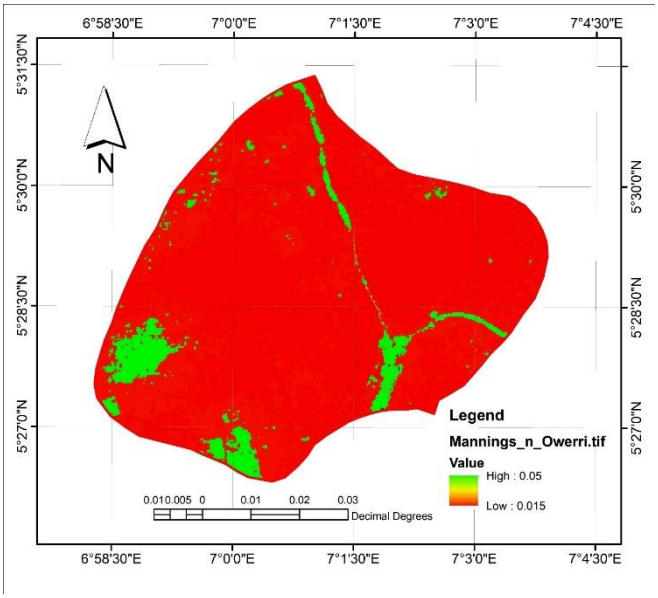

Figure 2: Manning's n values showing areas of low and high resistance

Table 5: Manning's n values showing areas of low, moderate and high resistance

Coverage	Area (km²)	Percentage (%)
Low Resistance	35.29	61.07
Moderate Resistance	18.62	32.21
High Resistance	3.88	6.72

Figure 2 and Table 5 presents the aggregated distribution of surface roughness across Owerri Municipal based on Manning's roughness coefficient (n) classifications. The spatial classification of Manning's roughness coefficients (*n*) across Owerri Municipal revealed varying levels of surface resistance to overland flow, which were categorized into low, moderate, and high resistance zones. This classification was based on the underlying land cover types and their respective hydraulic properties, and it forms a crucial basis for understanding the hydrodynamic behavior of the urban landscape under flood conditions.

The low resistance zone, corresponding to Manning's *n* values ranging from approximately 0.015 to 0.020, occupies an area of 35.29 km², which accounts for 61.07% of the total study area. This category includes primarily built-up areas (n = 0.015) and bare land (n = 0.020). Built-up areas are characterized by impervious surfaces such as concrete pavements, rooftops, and asphalt roads, which allow minimal water infiltration and facilitate rapid surface runoff. Similarly, bare land—comprising cleared plots, exposed soil, and sandy areas—contributes to quick runoff generation due to the absence of vegetation cover and compaction of surface materials. The large extent of these low-resistance surfaces highlights the highly urbanized and impervious nature of Owerri, which, in turn, significantly increases its susceptibility to flash flooding during heavy rainfall events.

In contrast, the moderate resistance zone, with a representative Manning's *n* value of approximately 0.035, covers an area of 18.62 km² or 32.21% of the total landscape. This zone is dominated by water bodies, including slow-flowing rivers such as the Otamiri and Nworie Rivers, as well as drainage channels and seasonal wetlands. Although these surfaces exhibit moderate flow resistance, especially in shallow or vegetated reaches, they play a critical dual role in the flood hydrology of the area. On one hand, they facilitate downstream conveyance of floodwaters in channelized sections; on the other, they function as temporary flood storage zones, particularly in low-lying depressions, helping to attenuate flood peaks and delay runoff delivery.

The high resistance zone, characterized by a Manning's *n* value of approximately 0.050, represents areas covered by vegetation such as grasslands, shrubs, parks, and riverine buffers. This class accounts for only 3.88 km², or 6.72% of the total area—making it the smallest category in terms of spatial coverage. Despite its limited extent, this zone is hydrologically significant due to the role of vegetation in increasing surface roughness, enhancing water infiltration, reducing flow velocity, and promoting sediment deposition. These vegetated areas serve as important ecological buffers and help to stabilize soils, reduce erosion, and regulate local microclimates, particularly around riparian corridors.

The classification and spatial distribution of Manning's roughness values provide valuable insight into the flood response dynamics of Owerri Municipal, particularly in relation to runoff generation, flow velocity, and inundation extent during storm events.

One of the most notable implications of the findings is the high urban flood risk associated with the dominance of low-resistance surfaces. With over 60% of the municipal area exhibiting minimal resistance to flow, there is a heightened potential for rapid surface runoff, shortened time-to-peak discharge, and limited natural water retention capacity. This pattern exacerbates the likelihood and severity of flash flooding, particularly in urban corridors with poor or inadequate drainage infrastructure.

Furthermore, the results point to a limited presence of vegetative buffer zones, as evidenced by the small proportion of high-resistance surfaces. The presence of only 6.72% vegetation-covered area indicates significant environmental degradation and the continued encroachment of built-up development into natural spaces. This loss of green infrastructure diminishes the system's capacity to naturally regulate stormwater and contributes to increasing urban vulnerability.

From a planning and engineering perspective, the spatial mapping of these resistance zones presents an opportunity for targeted intervention and policy development. For instance, urban planners and environmental engineers can prioritize the integration of green infrastructure solutions—such as permeable pavements, green roofs, urban parks, and vegetated swales—into low-resistance zones to improve surface retention, reduce flow velocity, and enhance urban resilience to flooding.

Lastly, the stratification of roughness values across the landscape contributes to the calibration and accuracy of hydraulic models, particularly those developed in HEC-RAS 2D. By integrating spatially distributed Manning's *n* coefficients, the model achieves greater realism in simulating flood behavior, including water surface elevations, inundation depth, and flood extent. This, in turn, enhances the predictive power and decision-support capacity of the model, enabling more effective flood management and emergency planning.

3.3. Surface Runoff Potential Analysis Using the SCS-Curve Number Method

To assess the surface runoff response of Owerri Municipal, the Soil Conservation Service Curve Number (SCS-CN) method was applied using integrated spatial datasets, including land use/land cover, hydrologic soil groups (HSGs), and rainfall data. A standard rainfall depth of 75 mm was adopted to simulate a moderate storm event commonly associated with seasonal rainfall intensities in southeastern Nigeria.

The curve number values (CN) were derived by cross-referencing the classified land cover types with the resampled soil hydrologic group raster, following standard SCS guidelines. Built-up areas with low permeability and compacted soils (HSG D) were assigned higher CN values (94), while vegetation-covered areas on more permeable soils (HSG B or C) received lower CN values (61–74), reflecting their increased capacity for infiltration and reduced runoff generation.

Following the generation of the CN raster, the potential maximum retention (S) was computed for each pixel, and subsequently, the direct runoff depth (Q) was estimated using the standard SCS-CN runoff equation. The result was a spatially distributed runoff depth raster representing the expected surface runoff response across the study area, see figure 3.

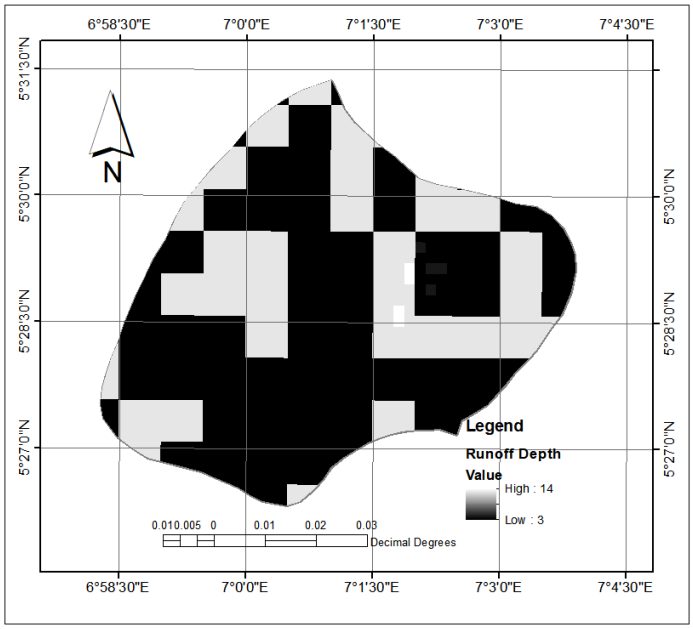

Figure 3: Runoff Depth Raster

The analysis revealed a mean runoff depth of approximately 45.32 mm, indicating that a significant portion of the rainfall event contributes to overland flow rather than infiltration or evapotranspiration. The maximum runoff depth recorded was 49.30 mm, primarily concentrated in densely built-up zones with high impervious surface coverage and compacted soils—conditions that severely limit infiltration and promote rapid runoff. Conversely, minimum runoff depths of 0 mm were observed in localized areas such as water bodies or well-vegetated patches with moderate-to-high infiltration capacity. These zones likely served as natural depressions or recharge areas capable of absorbing rainfall without generating surface flow.

The results are consistent with the land cover pattern previously established, where over 61% of the municipal area was classified as built-up or bare land, characterized by low surface roughness and minimal water retention potential. This land cover distribution, combined with the predominance of hydrologic soil groups C and D, significantly amplifies the risk of stormwater accumulation and surface flooding.

From a hydrological perspective, the high mean runoff depth implies that urban flooding is likely to occur even under moderate rainfall conditions, especially in areas where drainage infrastructure is insufficient or poorly maintained. This underscores the need for integrating green infrastructure, such as vegetated swales, permeable pavements, and urban green spaces, into flood management strategies to enhance infiltration and reduce runoff volumes.

Furthermore, the spatial runoff map generated from this analysis serves as a valuable decision-support tool for urban planners and disaster risk managers. It enables the identification of high runoff zones, supports the prioritization of flood-prone areas for intervention, and improves the accuracy of subsequent hydraulic modeling and flood vulnerability assessments.

3.4. Flood Vulnerability Modeling Using Rain-on-Grid Simulation

In an effort to quantitatively assess the spatial extent and severity of flood vulnerability within Owerri Municipal, a two-dimensional hydraulic flood modeling approach was implemented using a rain-on-grid simulation technique. This simulation was conducted using three primary datasets: a Digital Elevation Model (DEM) for terrain representation, a spatially distributed Manning's roughness coefficient raster derived from land cover characteristics, and an extreme rainfall input of 3391.2 mm, which represents a hypothetical worst-case scenario based on accumulated extreme precipitation conditions. The intent of this simulation was to model the municipality's hydrological response to a high-intensity rainfall event, particularly within the context of urban expansion and climate change-induced flood risks.

The rainfall event was converted into surface runoff volume using the SCS-Curve Number (SCS-CN) method, which accounts for both land use/land cover and soil infiltration capacity. The resulting runoff depth was then distributed spatially across the study area and routed using the terrain's slope characteristics. This rain-on-grid approach enabled the model to simulate overland flow dynamics without requiring predefined channel flow paths, making it particularly suitable for urban catchments with complex drainage behavior and undocumented sub-surface flow pathways.

The simulation produced a flood depth raster that revealed considerable variation in water accumulation across the municipality. As expected, floodwater tended to concentrate in areas of gentle slope, terrain depressions, and zones lacking sufficient surface drainage infrastructure. These are characteristic of many rapidly urbanizing environments where impervious surfaces have proliferated without proportional investments in flood management infrastructure, see figure 4.

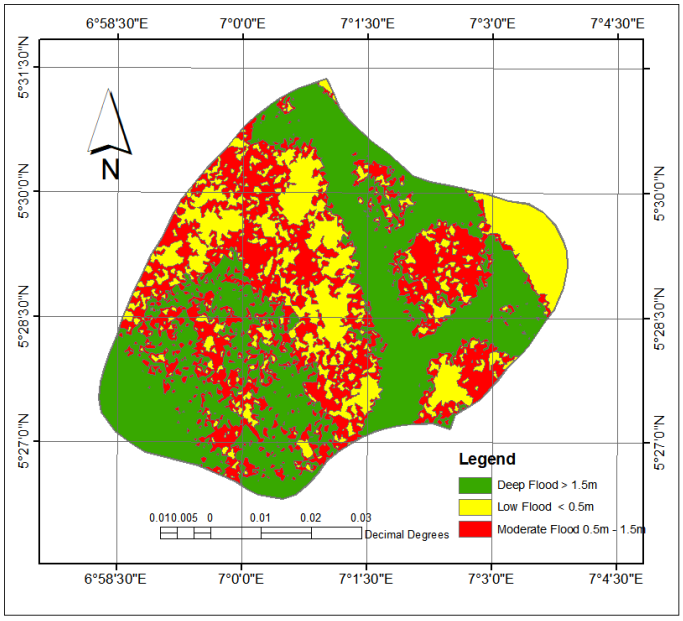

Figure 4: Flood Depth Raster

To better interpret the potential risk, the simulated flood depths were classified into three distinct flood vulnerability categories based on standardized depth thresholds:

1. Low vulnerability, these are flood depths ranging from 0 to 500 mm, typically indicative of shallow inundation with minimal impact on structures or movement.

2. Moderate vulnerability, these are depths between 501 and 1500 mm, representing significant ponding that may disrupt vehicular movement, damage properties, or inundate low-lying buildings.

3. High vulnerability, these are depths greater than 1500 mm, representing deep and hazardous flooding conditions with the potential to cause widespread structural damage, displacement of residents, and disruption of critical services.

The results of the classification indicated that a significant portion of Owerri Municipal falls within the moderate to high vulnerability classes. Low vulnerability zones were found in relatively elevated or well-drained areas, where terrain slope and permeable surfaces facilitate efficient runoff dispersion or infiltration. These areas may include naturally vegetated regions and portions of urban developments with adequate stormwater infrastructure.

Moderate vulnerability zones were distributed throughout semi-urban neighborhoods and peri-urban zones, especially where transition between built-up and vegetated land occurs. These areas are often partially impervious and lack formal drainage systems, rendering them susceptible to flooding during prolonged or high-intensity rainfall events.

High vulnerability zones were predominantly concentrated in topographic depressions, river floodplains, and highly developed urban cores. These regions are marked by low infiltration capacity due to concrete paving, building density, and limited drainage infrastructure. Consequently, they are at significant risk of deep and prolonged inundation, posing threats to residential areas, transportation corridors, and public utilities.

The maximum simulated flood depth was found to be approximately 3354.21 mm, which correlates closely with the total runoff volume generated from the extreme rainfall input. The mean flood depth across the study area was estimated at 536.63 mm, indicating a widespread potential for damaging flood conditions, particularly in built-up zones and poorly drained urban basins. The presence of shallow to moderately deep flooding across large areas highlights the limited hydrological resilience of Owerri's built environment to intense storm events.

These results underscore the urgency of integrating proactive flood mitigation measures into urban development policies. Such measures may include the deployment of stormwater detention and retention structures, the creation of flood-safe zones, the restoration of urban wetlands and natural drainage corridors, and the enforcement of land use zoning regulations that restrict construction within known flood-prone zones.

The rain-on-grid flood vulnerability modeling provided a clear evidence of Owerri Municipal's high exposure to extreme rainfall-induced flooding. The findings serve as a critical decision-support tool for urban planners, policymakers, and disaster risk managers, supporting the design of climate-resilient infrastructure and sustainable urban flood management frameworks.

3.4.1. Analysis of Landcover Exposure to Flood Vulnerability

To understand the distribution of flood impacts across different land use types in Owerri Municipal, a spatial overlay analysis was conducted between the classified flood vulnerability zones and land cover/land use (LULC) data. The exposure analysis revealed how varying land cover categories—namely Built-Up Areas, Bare Land, Vegetation, and Water Bodies—correspond to low, moderate, or high flood vulnerability zones.

The results indicated that Built-Up Areas were the most exposed to flooding, with a total of approximately 1391.90 hectares falling within high vulnerability zones, 1221.50 hectares in moderate vulnerability zones, and 879.73 hectares in low vulnerability zones. This pattern indicates that dense urban infrastructure in Owerri, characterized by impervious surfaces and poor drainage systems, significantly amplifies surface runoff and contributes to urban flood risks.

Bare Land was also notably exposed, with 939.92 hectares categorized as highly vulnerable, 560.31 hectares as moderately vulnerable, and 387.52 hectares as low vulnerability. These areas typically represent undeveloped

plots, cleared land for construction, or transitional urban spaces that lack vegetation cover. Their exposure emphasizes the role of land disturbance and absence of protective vegetation in increasing susceptibility to flood accumulation.

Vegetation-covered areas, though generally considered natural buffers to flood risk, still accounted for 201.53 hectares within high vulnerability zones, 67.95 hectares in moderate zones, and 19.26 hectares in low vulnerability areas. This indicates that despite their hydrological benefits, some vegetated zones are situated in low-lying or poorly drained parts of the city, making them susceptible to waterlogging during intense storms.

Water Bodies, including rivers, ponds, and drainage basins, were naturally located in flood-prone areas. About 162.25 hectares of water surfaces were categorized within high flood vulnerability zones, while 4.24 hectares and 0.63 hectares were classified under moderate and low vulnerability, respectively. These zones serve both as conduits for floodwater and as flood hazards when capacity is exceeded, see table 6.

Table 6: Land Cover Exposure by Flood Vulnerability

Landcover	Low Vulnerability (ha)	Moderate Vulnerability (ha)	High Vulnerability (ha)
Built-Up	879.73	1221.50	1392.20
Bare Land	387.52	560.31	947.11
Vegetation	19.26	67.95	284.91
Water Body	0.63	4.24	162.25

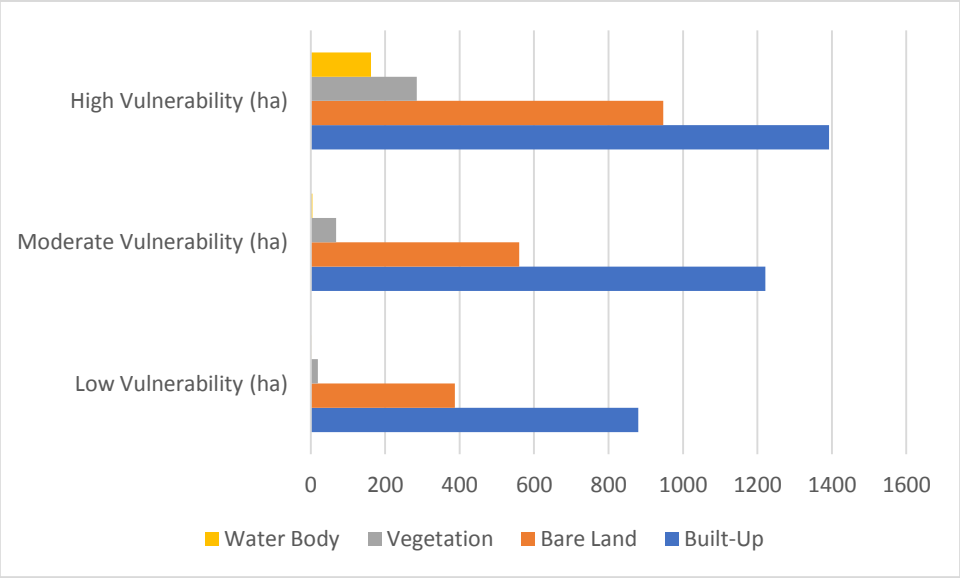

Figure 5: Land Cover Exposure by Flood Vulnerability Distribution

The prevalence of Built-Up areas and Bare Land within high flood vulnerability zones in Owerri Municipal provides compelling evidence of the significant influence of anthropogenic activities on flood risk dynamics. The concentration of built-up zones—comprising roads, residential housing, commercial structures, and impermeable surfaces—in flood-prone areas limits the infiltration of rainfall, accelerates surface runoff, and

overwhelms existing drainage systems. Similarly, Bare Land, often representing construction sites, cleared plots, or undeveloped tracts devoid of vegetation, contributes to flood susceptibility by exposing the soil to erosion and minimizing the landscape's capacity to absorb stormwater.

Although vegetation has traditionally been regarded as a natural buffer against flooding, its spatial coverage within the study area is notably limited. The exposure of vegetated zones to high vulnerability levels in certain parts of the municipality suggests that even green areas are not immune to flooding—particularly when situated in topographic depressions, poorly drained basins, or alongside natural watercourses. This underscores the need to consider not just land cover type but also topographic and hydrological context in urban flood risk assessments.

Water bodies, including rivers, streams, and man-made reservoirs, serve a dual hydrological function. On one hand, they act as conduits and temporary storage systems that help attenuate surface runoff during rainfall events. On the other hand, when capacity thresholds are exceeded or channels are blocked, these features become sources of overflow and inundation, posing direct threats to adjacent communities. Their location in high vulnerability zones reinforces the importance of regular maintenance, dredging, and monitoring of drainage channels and floodplains.

These findings collectively highlight the critical need for integrated urban flood management strategies. Urban development must be guided by policies that prioritize ecological preservation alongside infrastructural expansion. This includes enforcing zoning regulations that prevent indiscriminate construction in floodplains, investing in climate-resilient drainage infrastructure, and promoting the establishment of urban green infrastructure—such as parks, permeable pavements, bioswales, and reforested corridors. By embedding flood mitigation into land use planning, Owerri Municipal can significantly enhance its resilience to extreme hydrometeorological events and protect both people and property from the escalating threat of urban flooding.

3.4.2. Road Network Exposure to High Flood Vulnerability Zones

The road network represents a critical component of urban infrastructure, serving as the primary medium for mobility, commerce, emergency response, and connectivity. In this study, an overlay analysis was conducted to assess the extent to which different road classes in Owerri Municipal intersect with areas classified as high flood vulnerability zones. The results offer valuable insights into the susceptibility of the transport network to inundation during extreme rainfall events.

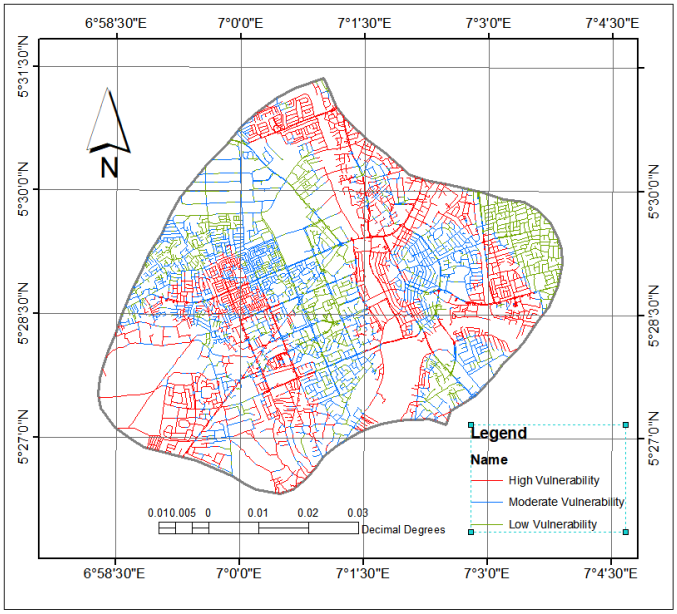

Figure 6: Road Network Exposure by Flood Vulnerability

A total of 43 road segments were identified as being located within high flood vulnerability zones. These segments were grouped according to their functional classification—namely residential, primary, trunk, secondary, tertiary, and unclassified roads. The cumulative length (in meters) of each category exposed to high flood risk is presented in Table 7.

Table 7: Road Exposure to High Flood Vulnerability Zones in Owerri Municipal

Road Class	Total Length Exposed (m)
Residential	8,122.21
Primary	4,400.02
Trunk	3,723.01
Secondary	2,463.49
Tertiary	1,235.92
Trunk Link	59.19
Unclassified	8.54
Total	20,012.38

The findings indicate that residential roads represent the largest share of exposure, with a combined length of approximately 8.12 kilometers located within high flood risk zones. This reflects the rapid urban expansion and the development of residential neighborhoods in poorly drained low-lying areas. Roads such as 7th Avenue, 10th Avenue, and Obinze-FUTO Road are particularly vulnerable and are frequently reported to experience severe waterlogging during heavy rainfall.

Primary roads, including key transportation corridors like the Port Harcourt – Owerri Road, were also found to be significantly affected, with 4.4 kilometers of exposed segments. These roads serve as the main arteries of inter-city and regional travel, and their inundation poses serious threats to economic continuity, emergency response efficiency, and regional connectivity.

The trunk road network, which includes the Aba – Owerri Road, is another critical class at risk, contributing over 3.72 kilometers of exposed road segments. These roads carry heavy traffic and are essential for logistics and trade. Flooding in these corridors can result in substantial socio-economic losses and prolonged delays in goods movement.

The secondary and tertiary road networks also show considerable vulnerability, with 2.46 km and 1.24 km of exposed segments, respectively. These roads are essential for intra-urban movement and provide access to residential areas, schools, health centers, and commercial zones. Recurrent flooding along these roads could isolate communities, obstruct access to essential services, and hinder daily life for residents.

Lastly, trunk link and unclassified roads, while minimal in total length, still require consideration, especially in areas where they connect to critical facilities or act as service roads for high-density zones.

3.4.3. Road Network Exposure to Moderate Flood Vulnerability Zones

Moderate vulnerability zones represent transitional flood-prone areas—regions that may not flood frequently but are still at risk during high-intensity storms or prolonged rainfall events. Understanding the spatial relationship between these zones and the road network is critical for improving infrastructure resilience and planning alternate access routes during emergencies. The cumulative length (in meters) of each category exposed to moderate flood risk is presented in Table 8.

Table .8: Road Exposure to Moderate Flood Vulnerability Zones

Road Class	Total Length Exposed (m)
Tertiary	8,940.82
Residential	6,899.40
Secondary	5,129.42
Trunk	6,022.64
Primary	2,862.17
Unclassified	1,669.91
Total	31,524.36

The analysis reveals that tertiary roads represent the largest class of roads exposed to moderate flood vulnerability, accounting for over 8.9 kilometers of road length. These roads include vital connectors such as Tetlow Road, Ikenna Nzimiro Avenue, Ellen Sirleaf Road, Concorde Avenue, and Musa Yar'Adua Way, which play important roles in neighborhood-level accessibility and service delivery.

Residential roads also show significant exposure, with a total of 6.9 kilometers intersecting moderate flood zones. Streets like Winners Chapel Crescent, Dr. Gideon Nweze Avenue, and Orio Avenue exemplify the risk faced by densely populated neighborhoods.

Secondary roads, such as Sam Mbakwe Avenue, Akachi Road, and Wetheral Road, account for approximately 5.1 kilometers, highlighting their exposure despite being critical urban transport corridors.

Trunk and primary roads have combined exposures of over 8.8 kilometers, suggesting that even higher-grade roads like Port Harcourt – Owerri Road and Aba – Owerri Road are not immune to moderate flood impacts, which may disrupt inter-city and freight transport operations.

3.4.4. Road Network Exposure to Low Flood Vulnerability Zones

This section presents the analysis of roads within low flood vulnerability zones in Owerri Municipal. While these areas face a lower risk of severe inundation, understanding their exposure remains important for resilience planning and maintaining continuity during moderate rainfall events.

A total of over 65 unique road segments intersects with low vulnerability zones. The total length exposed, grouped by road class, is summarized in Table 9.

Table .9: Road Exposure to Low Flood Vulnerability Zones

Road Class	Total Length Exposed (m)
Residential	3,314.69
Secondary	3,073.34
Tertiary	5,429.83
Trunk	5,670.69
Primary	1,297.61
Unclassified	1,730.06
Total	20,516.22

The analysis shows that tertiary and trunk roads account for the largest portion of roads within low vulnerability areas—suggesting that some important routes, including Onitsha–Owerri Road and Concorde Avenue, fall in relatively flood-safe terrain. These routes may serve as alternate access corridors during heavy storm events when other segments are submerged.

Residential roads, with over 3.3 kilometers of their length located in low vulnerability zones, suggest that several neighborhoods—such as World Bank Estate and Dr. Gideon Nweze Avenue—are situated in better-drained areas or on higher ground. These locations may serve as refuge zones or critical nodes for evacuation staging during severe flood events.

However, the presence of over 3 km of secondary roads in these zones, including Sam Mbakwe Avenue, Wetheral Road, and Akachi Road, indicates that key intra-urban access routes retain some resilience but still require flood preparedness due to their functional importance.

4. Conclusion

This study successfully employed a geospatial and hydraulic modeling approach to predict flood inundation across Owerri Municipal, Imo State, with emphasis on spatial land cover analysis, surface runoff estimation, and vulnerability zoning. The findings address each research objective and provide critical insight into the flood dynamics of the study area.

The land cover/land use analysis revealed that built-up areas (61.07%) dominate the landscape, significantly reducing the natural capacity of the land to absorb rainfall. Vegetation and water bodies, which aid infiltration and natural flood mitigation, are critically underrepresented.

The assignment and mapping of Manning's roughness coefficients across the study area showed that more than 61% of the terrain exhibits low surface resistance, allowing fast surface runoff and promoting the rapid spread of floodwaters.

Surface runoff modeling using the SCS-Curve Number method indicated that the region is highly prone to runoff generation, especially during extreme rainfall events. The simulation for a 3391.2 mm rainfall event demonstrated a mean runoff depth of 536.63 mm, highlighting the susceptibility of the area to surface flooding.

The HEC-RAS 2D rain-on-grid simulation identified spatially distinct flood vulnerability zones. High vulnerability zones were predominantly located in low-lying, densely built-up areas and river corridors, while moderate zones appeared in transitional urban areas with mixed permeability. Low vulnerability zones were associated with elevated or vegetated terrains.

Exposure analysis showed that critical land cover classes and road infrastructure are significantly affected. Over 3,900 hectares of land—including residential, bare, and vegetated areas—lie within flood-prone zones. More than 20 km of roads are exposed to high vulnerability, with an additional 31 km in moderate zones, threatening both mobility and access to emergency services.

These conclusions underscore the impact of urban expansion, poor land use planning, and inadequate drainage on flood risks in Owerri Municipal. The study provides a decision-support framework that integrates land surface parameters and hydraulic modeling for better flood risk planning and infrastructure management.

References

Adedeji, O. H., Odufuwa, B. O., & Adebayo, O. H. (2012). Building capabilities for flood disaster and hazard preparedness and risk reduction in Nigeria: Need for spatial planning and public education. *Journal of Sustainable Development in Africa*, 14(1), 45–58.

Adger, W. N., Brooks, N., Bentham, G., Agnew, M., & Eriksen, S. (2005). New indicators of vulnerability and adaptive capacity. *Tyndall Centre Technical Report No. 7*.

Adelekan, I. O. (2010). Vulnerability of poor urban coastal communities to flooding in Lagos, Nigeria. *Environment and Urbanization*, 22(2), 433–450.

Aderogba, K. A. (2012). Global warming and challenges of floods in Lagos metropolis, Nigeria. *International Journal of Sustainable Development*, 5(1), 79–91.

Adeoye, N. O., Ayanlade, A., & Babatimehin, O. (2009). Climate change and menace of floods in Nigerian cities: Socio-economic implications. *Advances in Natural and Applied Sciences*, 3(3), 369–377.

Ajibade, I., McBean, G., & Bezner-Kerr, R. (2013). Urban flooding in Lagos, Nigeria: Patterns of vulnerability and resilience among women. *Global Environmental Change*, 23(6), 1714–1725.

Bates, P. D., & De Roo, A. P. J. (2000). A simple raster-based model for flood inundation simulation. *Journal of Hydrology*, 236(1–2), 54–77.

Di Baldassarre, G., Schumann, G., Bates, P. D., Freer, J. E., & Beven, K. J. (2009). Flood-plain mapping: A critical discussion of deterministic and probabilistic approaches. *Hydrological Sciences Journal*, 55(3), 364–376.

Douglas, I., Alam, K., Maghenda, M., McDonnell, Y., McLean, L., & Campbell, J. (2008). Unjust waters: Climate change, flooding and the urban poor in Africa. *Environment and Urbanization*, 20(1), 187–205.

Efe, S. I. (2011). Spatial variation of rainfall amount and pattern in the Niger Delta region, Nigeria. *Journal of Geography and Geology*, 3(1), 10–20.

Fonstad, M. A., Dietrich, J. T., Courville, B. C., Jensen, J. L., & Carbonneau, P. E. (2013). Topographic structure from motion: A new development in photogrammetric measurement. *Earth Surface Processes and Landforms*, 38(4), 421–430.

Horritt, M. S., & Bates, P. D. (2002). Evaluation of 1D and 2D numerical models for predicting river flood inundation. *Journal of Hydrology*, 268(1–4), 87–99.

Ishaya, S., Ifatimehin, O. O., & Okafor, C. (2009). Remote sensing and GIS applications in flood risk analysis: A case study of River Benue floodplain, Nigeria. *African Journal of Environmental Science and Technology*, 3(5), 109–117.

Jonkman, S. N. (2005). Global perspectives on loss of human life caused by floods. *Natural Hazards*, 34(2), 151–175.

Kundzewicz, Z. W., Kanae, S., Seneviratne, S. I., Handmer, J., Nicholls, N., Peduzzi, P., ... & Sherstyukov, B. (2014). Flood risk and climate change: Global and regional perspectives. *Hydrological Sciences Journal*, 59(1), 1–28.

Mandlburger, G., Pfennigbauer, M., Pfeifer, N., Rieger, P., & Ullrich, A. (2015). Airborne hydrographic LiDAR mapping—potential and limitations. *Remote Sensing*, 7(1), 146–179.

Nwilo, P. C., Olayinka, D. N., & Anifowose, A. Y. B. (2012). Urban flood modeling in Nigeria using remote sensing and GIS. *Disaster Risk Management Journal*, 4(2), 112–123.

Ologunorisa, T. E., & Abawua, T. J. (2005). Flood risk assessment: A review. *Journal of Environmental Studies*, 1(1), 35–42.

Pereira, S., Zezere, J. L., Bateira, C., & Tavares, A. O. (2017). Landslide susceptibility mapping in a lowland area using probabilistic and deterministic models. *Geomorphology*, 298, 12–24.

Teng, J., Jakeman, A. J., Vaze, J., Croke, B. F. W., Dutta, D., & Kim, S. (2017). Flood inundation modeling: A review of methods, recent advances, and uncertainty analysis. *Environmental Modelling & Software*, 90, 201–216.